applied sciences

*Article*

# Sustainable Approach of Generating Water and Energy: Techno-Economic Analysis of a Hybrid Solar Photoactive Thermal System Coupled with Direct Contact Membrane Distillation for Water Purification and Electricity Generation

**Fahad Awjah Almehmadi [1], Abdullah Najib [2], Emad Ali [3,*], Hany Al-Ansary [2] and Jamel Orfi [2]**

1 Department of Applied Mechanical Engineering, College of Applied Engineering, Muzahimiyah Branch, King Saud University, P.O. Box 800, Riyadh 11421, Saudi Arabia
2 Mechanical Engineering Department, King Saud University, P.O. Box 800, Riyadh 11421, Saudi Arabia
3 Chemical Engineering Department, King Saud University, P.O. Box 800, Riyadh 11421, Saudi Arabia
* Correspondence: amkamal@ksu.edu.sa

**Citation:** Almehmadi, F.A.; Najib, A.; Ali, E.; Al-Ansary, H.; Orfi, J. Sustainable Approach of Generating Water and Energy: Techno-Economic Analysis of a Hybrid Solar Photoactive Thermal System Coupled with Direct Contact Membrane Distillation for Water Purification and Electricity Generation. *Appl. Sci.* **2022**, *12*, 9137. https://doi.org/10.3390/app12189137

Academic Editor: Yosoon Choi

Received: 26 July 2022
Accepted: 3 September 2022
Published: 12 September 2022



**Abstract:** Cogeneration of energy and clean water by incorporating direct contact membrane desalination (DCMD) and photovoltaic hybrid thermal system (PVT) into a residential building is a promising technology for addressing water and energy shortage in distant places. In this study, a microgrid integration between PVT, DCMD, and a residential building is proposed, with an end goal to meet partial electric load in the building and provide a clean water supply. A mathematical model was developed and validated to assess the system's performance. Artificial Neural Network (ANN) and optimization techniques have been used. The performance of the proposed system was studied under the meteorological conditions of Riyadh, Saudi Arabia, and under several design and operation parameters. The optimal performance of the system is found as functions of the inlet brackish water temperature to the PVT, capital and installation cost, and the desired water productivity. Results reveal that the specific cost of water (SCW) is 23.6 $\$/m^3$ achieved with a renewable energy penetration of 25%, depending on the cost of PVT and electricity price. Thus, the proposed system meets 25% of the electric demand for the residential building, while the rest is imported from the grid. In addition, the proposed system reduced the annual greenhouse gas emission by 4300 kg for a single building. This study will contribute to a better understanding of incorporating innovative clean energy and water systems such as PVT and DCMD into a residential house.

**Keywords:** sustainable energy; membrane distillation; photovoltaic hybrid thermal system

## 1. Introduction

Energy and water are precious resources and are essential for human well-being. Currently, around 759 million people lack access to energy [1], and 771 million do not have access to clean potable water [2]. The shortfall will widen owing to climate change and global population growth, which is anticipated to raise water and energy consumption by 50% and 100%, respectively, by 2050 [3]. The world's key supplies of energy and water are deteriorating and diminishing at an astounding level, which exacerbates this issue makes it even worse shortly. Even though desalination provides a long-term solution to compact the water shortage problem, most desalination procedures are energy-intensive which puts additional strain on the current energy supply. This necessitates the development of renewable-based, long-term desalination technologies, particularly in distant areas where energy generation from renewable sources has significant economic and environmental consequences.

Arab Gulf countries seek to decarbonize their energy sectors by shifting to clean energy [4]. The path to reduce the reliance on fossil fuels and decarbonize the energy sector is possible in the gulf regions due to massive solar energy resources. Saudi Arabia is among the top 15 countries globally that possess enormous potential in PV power generation [4]. With this, Saudi Arabia stated a clear goal to move away from conventional power generation plants that rely on fossil fuels to more sustainable options. Saudi Arabia aims to decarbonize half of the energy sector by boosting the renewable energy penetration by 2030 [5]. The transitions to renewable energy cannot be attained without addressing the high energy demand in the residential buildings and desalination industry, which consumes a large portion of the total energy produced in Saudi Arabia (KSA). Energy consumption for buildings in KSA accounts for 80% of the total electricity, with 50% consumed primarily by the residential sector [6]. In addition, energy consumption for desalination accounts for roughly 20% of the overall energy consumption [7].

A hybrid photovoltaic thermal energy system (PVT) is a promising technology that can provide heat and electricity, simultaneously. Due to the high sun radiance in water-scarce areas, solar energy is also an effective energy source for desalination. Most existing desalination systems, including multi-effect distillation (MED), reverse osmosis (RO), and membrane distillation (MD), may be powered by solar collectors either in form of electric energy, heat or both [8]. Among these technologies, direct contact membrane distillation (DCMD) has great potential due to its capability to be combined with low-grade solar thermal energy. For example, Krnac et al. experimentally investigated the possibility of integrating a concentered PVC with DCMD [9]. The results of the integrated system were promising, and their system was capable of generating power and purifying water simultaneously. Rahaoui et al. proposed a water desalination system that includes a DCMD and a solar pond [10]. Results show that increasing the feedwater temperature improved the produced water mass flux. Kim et al. proposed a solar-assisted direct contact membrane distillation (DCMD) system with unique energy recovery techniques that can operate 24 h a day [11]. The specific thermal energy usage in the proposed system was 43% lower as a result of utilizing heat recovery. Another study proposed by Shafieian et al. integrated a heat pipe solar system with DCMD [12]. The performance of their system was tested experimentally, and results indicated that the heat pipe solar system was capable of providing all of the required thermal energy for DCMD. In addition, a multivariable optimization technique of a combined solar power system with DCMD was presented by Karam et al. [13]. Chen et al. proposed a decentralized water/electricity cogeneration system using a vacuum multi-effect membrane distillation system assisted with a concentrated photovoltaic thermal system [14]. Results indicated that the solar collector cost and the electricity price have a tremendous effect on the specific cost of water $/m$^3$.

Among various desalination technologies, membrane distillation (MD) is a promising one because it operates at a lower temperature, often less than 100 °C. Several studies have been conducted on MD when it is integrated with other renewable energy such as solar energy [8,12]. One of the drawbacks of utilizing solar energy in MD technology is increasing the cost as compared with a conventional plant that uses fossil fuel. Among other sustainable energy sources, geothermal energy in MD is anticipated to lower the cost of producing water. For example, Fawzi and Nesreen proposed a small-scale solar-powered membrane distillation system for a rural area [15]. The cost of water in their study was 18 $/m$^3$. Another study proposed by Guopei and Lin investigated the performance of sweeping gas membrane distillation driven by solar energy for coastal households [16]. The proposed system aims for supplying island and coastal families with a flexible and consistently fresh water supply. Results show that the solar collector area has a great impact on the system's performance. The cost of desalinated water in their system was 18.34 $/m$^3$. Li and Guo performed economic and energy analysis of a hollow fiber membrane distillation powered by solar energy [17]. Results indicated that the cost of producing water is 16.88 $/m$^3$.

The rate of growth of energy demand and portable water will likely continue to rise due to population expansion. Thus, many studies were conducted recently aiming to develop an energy-efficient hybrid system that can provide a sustainable energy source for residential buildings and the desalination processes. For residential buildings for example, a techno-economic optimization of hydrogen power production by using solar and wind was proposed by Al-Sharafi et al. [18]. The proposed system had investigated different climate conditions in the Kingdom of Saudi Arabia. The minimum levelized cost of energy (LCOE) in the study was $1.208/kWh. Another study developed a combination of solar PV and wind hybrid energy system for residential buildings in four cities located in different climate zone in Saudi Arabia, namely, Yanbu, Sharurah, Hafar Albatin, and Riyadh [19]. The study results demonstrated that the proposed hybrid energy system is economically viable in Yanbu, attributable to high renewable energy penetration. The main contribution of this study was reducing greenhouse gases as well as lowering energy costs. Furthermore, an evaluation and techno-economic design of a hybrid energy system for residential buildings communities in Jubail were investigated by Baseer et al. [20]. This hybrid energy system comprises PV/Wind/Diesel and PV/Wind with battery storage with an end goal to meet the electric load demands for three housing compounds. Using HOMER software, the technical and economic feasibility of different configurations has been evaluated. The minimum average LCOE for three compounds was $0.217/kWh. The minimum LCOE was $0.25/kWh for PV and wind turbine, coupled with energy storage, that provides 100 percent renewable energy penetration. Moreover, the ideal proposed system estimated to save 2800 tons of carbon dioxide annually. In addition, a hybrid system that consisted of Solar PV, WT, and a diesel generator was designed for a village in Saudi Arabia [21]. The proposed hybrid system expected to replace eight diesel types that were generated to meet the village's electric loads. The optimized results show that the energy cost is $0.212/kWh with 35% renewable energy penetration. Other studies minimized energy usage in a residential building using phase change material (PCM). Results from these studies revealed that energy usage associated with air conditioning dropped by 43.2% [22,23].

A cogeneration system that aims to decentralize water/electricity is proposed in this study. The proposed system incorporates a direct contact membrane desalination unit and PVT into a typical residential building. A mathematical model is developed to estimate the performance of the system based on the metrological climate conditions for the city of Riyadh, Saudi Arabia. Various design parameters that affect the cost of water and electricity were investigated. The study's novelty is: (i) a sustainable cogeneration system was proposed to provide potable water and clean energy to residences; (ii) the rejected condenser water from the DCMD is used as regenerative hot water stream to run a small absorption chiller; (iii) in-depth techno-economic analysis is presented using in particular the Artificial Neural Network (ANN) algorithm.

## 2. System Description

A photovoltaic/thermal hybrid (PVT) powered system is a reliable source of energy where heat and electricity can be generated simultaneously. The proposed hybrid system shown in Figure 1 comprises primarily of PVT, a direct contact membrane desalination unit (DCMD) for water purification, a small absorption chiller, and a typical residential unit. The heat generated from the PVT ($H_1$) is used to heat the working fluid (i.e., Brackish water). In this case, the brackish water is heated in PVT before it enters the DCMD unit. The storage tank is used to collect the heated water and auxiliary heating is utilized if the temperature in the tank drops below 70 °C to ensure a constant energy source for the DCMD. The heat rejected from DCMD ($c_2$) is used as a regenerative source for a small-scale absorption chiller. Cold feed water obtained from the absorption chiller ($c_1$) is pumped to DCMD.

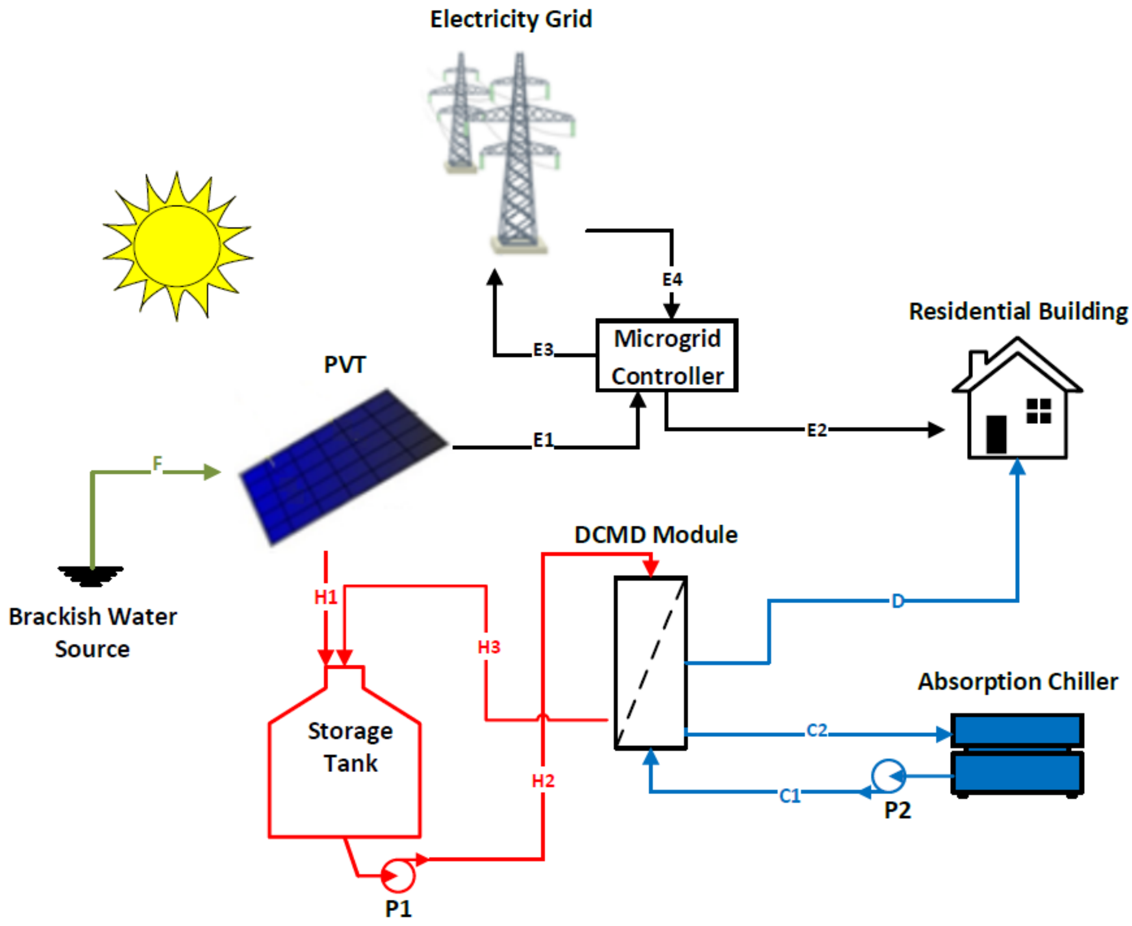


**Figure 1.** Conceptual diagram of the proposed system.

The electric energy generated by PVT ($E_1$) is used to cover the partial load of a residential building. If the electric energy produced by the PVT exceeds house electric demand, the extra energy will be sold to the local grid ($E_3$). Power imported from the grid ($E_4$) is used when the PVT is not capable of meeting the house's load.

## 3. Mathematical Model

A detailed mathematical model was developed to investigate the performance of the proposed system. The following assumptions have been made to solve the governing equations presented in this section:

I. the heat losses from the solar field and other components were neglected.
II. the residential building considered in this study has access to the grid.
III. the desalinated water might be brackish groundwater located near the house or recycling grey water.
IV. A water pump is used to transport water to the house.

### *3.1. DCMD Unit*

In this study, a Direct Contact Membrane Distillation (DCMD) module with an effective surface area of 10 m$^2$, 230 µm membrane thickness, 14 m channel length, 0.7 m channel height, 0.2 µm pore diameter, and 2 mm channel gap unit made by SolarSpring [24] is depicted in Figure 2. The input parameters in the experiment are illustrated in Figure 2. The evaporative hot stream temperature varies between 40 and 80 °C, and the volume flow rate should be in the range between 0–300 Lit/h. The mass flux production ranges between 0 to 1.9 kg/m$^2$·h.

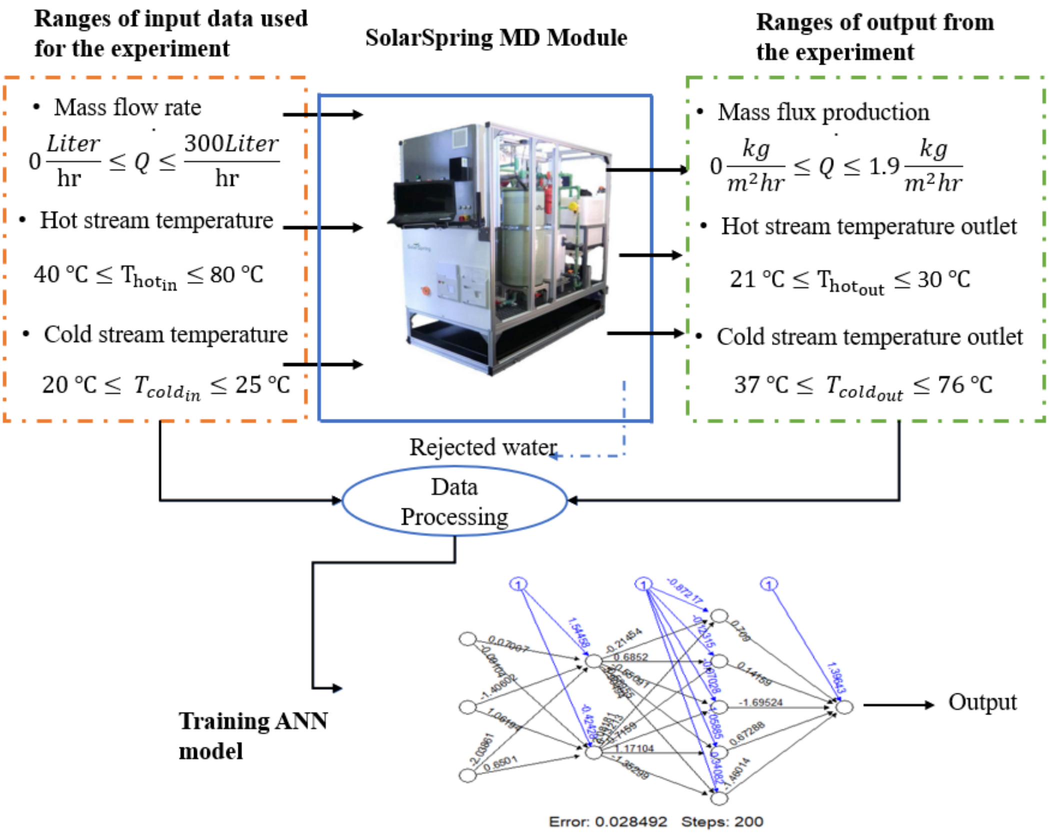


**Figure 2.** Artificial Neural Network.

Inspired by the experimental and theoretical studies by previous works [25,26], a machine learning algorithm, namely, Artificial Neural Network is developed to estimate the performance of the DCMD. The experimental dataset used to train the ANN model was illustrated in a previous study [26]. The developed DCMD's ANN model is shown in Figure 2. The input dataset was normalized to a range of (0,1). Then, the input parameters were divided into two parts: where 70% of data was used to train the ANN model, while 20% was utilized for testing. The ANN model of the DCMD was developed using R software [27]. The developed ANN model is valid to forecast the outputs, which are the hot and cold stream temperature and the water productivity, within the data ranges shown in Figure 2.

### 3.2. Hybrid Photovoltaic Thermal System

Desalination of seawater or brackish water is mostly powered by fossil fuels, which raises questions regarding greenhouse gas emissions, especially in the dry Middle East. There have been several initiatives to use solar resources to solve this problem, but all of them have focused on turning solar energy into electricity. To overcome these difficulties, previous research proposed a small-scale hybrid photovoltaic/thermal (PVT) solar collector-powered reverse osmosis (RO) desalination system suitable for a rural village in the Kingdom of Saudi Arabia (KSA) was constructed, and its power needs were estimated [28]. The PVT model developed previously in prior research was utilized in this work.

The type of PVT considered here is a flat-plate collector. A cross-section area of a typical flat-plate collector is shown in Figure 3, where I indicates the solar radiation falling on the collector's surface.

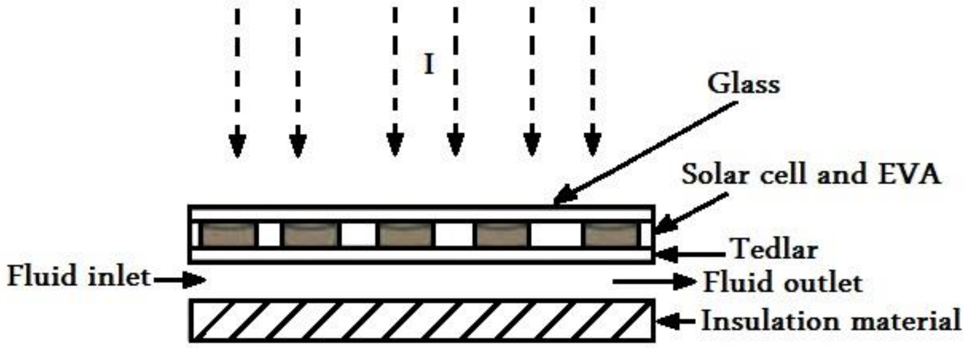


**Figure 3.** Block diagram for the PVT [28].

The governing equations of the PVT model that are used to predict electric and thermal energy generation were adopted from the literature [29,30]. The estimated array is made up of collectors wired in parallel $N_p$ and $N_s$ collector in series, totaling $N_p * N_s$ panels. Equation (1) is used to estimate the total thermal energy $(Q_h)$ transfer to the fluid from a connected series panel [30].

$$\dot{Q}_{h,\ total} = N_p * \dot{Q}_{h,N_s} \tag{1}$$

The thermal energy transmitted to the working fluid through $N_s$ panels connected in series is estimated by Equation (2), as follows [29]:

$$\dot{Q}_{h,N_s} = N_s A_c F_R \left( S \left[ \frac{1-(1-K_K)^{N_S}}{N_S K_K} \right] - U_L \left[ \frac{1-(1-K_K)^{N_S}}{N_S K_K} \right] \left( T_{fi} - T_a \right) \right) \tag{2}$$

The expression $K_k$ is given by [29]:

$$K_k = \frac{A_C F_R U_L}{m C_p} \tag{3}$$

In Equation (3), the fluid mass flow rate is denoted by m and the fluid specific heat is $C_p$. Equation (4) calculates the amount of solar radiation absorbed per unit area of a single PVT panel.

$$S = I(\alpha\tau)\left(1 - \frac{\eta_c}{\alpha}\right) \tag{4}$$

where $I$ refers to solar irradiation intensity, $\tau$ is the collector glazing transmittance. $\eta_c$ and $\alpha$ are the electric efficiency and the collector absorptance. The outlet temperature of the fluid is given by Equation (5) [29].

$$T_{fo} = \left[ \frac{S}{U_L} + T_a \right] \left[ 1 - e^{\left(-\frac{-N_s A_c F_R U_L}{m C_p}\right)} \right] + T_{fi} e^{\left(-\frac{-N_s A_c F_R U_L}{m C_p}\right)} \tag{5}$$

The following equation gives the collector heat removal factor [29]:

$$F_R = \frac{m c_p}{U_L} \left[ 1 - e^{-\frac{U_L \acute{F}}{m C_p}} \right] \tag{6}$$

Electric equations can be expressed as the following Equations (7) and (8) [28].

$$\dot{Q}_{e,total} = Q_e N_s N_p \tag{7}$$

$$Q_e = \frac{A_c S \eta_a}{\alpha} \left[ 1 - \frac{\eta_r B_r}{\eta_c} \left[ F_R \left( T_{fi} - T_a \right) + \frac{S}{U_L} (1 - F_R) \right] \right] \tag{8}$$

### 3.3. Storage Tank and Absorption Chillers

The storage tank is governed by the following energy balance equation. Equation (9) is derived based on the assumption that the water in the tank does not flow through the PVT array and only the brackish water flows through the PVT array to accumulate heat. To keep the tank temperature at the desired setpoint, the concept of the auxiliary heat $\dot{Q}_{aux}$ is described in [28].

$$C_p * V * \rho_w \frac{dT_{tank}}{dt} = \dot{M}_f C_p (T_f - T_{tank}) + \dot{Q}_{aux}(t) - \dot{\varnothing}_{losses}(t) \quad (9)$$

The multivariable polynomial model (MPR) developed by Labus et al. [31] is used to estimate the performance of the absorption chiller. The developed correlation model accurately calculates the absorption chiller's thermal loads.

$$Q_{evap} = B_0 + B_1 * Tgen_{in} + B_2 * Tac_{out} + B_3 * Teva_{in} + B_4 * Tgen_{in} * Tac_{out} + B_5 * Tgen_{in} * Teva_{in} + B_6 * Teva_{in} * Tac_{out} + B_7 * Tgen_{in}^2 + B_8 * Tac_{out}^2 + B_9 * Teva_{in}^2 \quad (10)$$

In Equation (10), the regenerative temperature is detonated by $T_{gen_{in}}$, condenser temperature is $Tac_{\ out}$ , and evaporative temperature is $Teva_{in}$. The output of Equation (10) $Q_{evap}$ is the cooling capacity of the chiller. The coefficients $(B_n)$ considered when calculating Equation (10) can be found in [31].

Table 1 shows the coefficients $(B_n)$ considered when calculating Equation (10).

**Table 1.** The coefficients $(B_n)$ used in Equation (10) [31].

| $B_0$ | $B_1$ | $B_2$ | $B_3$ | $B_4$ | $B_5$ | $B_6$ | $B_7$ | $B_8$ | $B_9$ |
|---|---|---|---|---|---|---|---|---|---|
| 6.818 | 0.3703 | −1.4329 | 1.113 | 0.0122 | 0.0014 | −0.0076 | −0.0025 | −0.0081 | −0.0217 |

### 3.4. Estimating Total Energy Consumption for a Residential Building

A model for the residential building is constructed in this section that can predict building heat gains/losses and related heating/cooling requirements with the external environment, as well as estimates of energy consumption from plug-in loads, such as lighting, and other equipment. This aims to estimate the hourly energy consumption, and to predict building heat losses/gains with the exterior environment to estimate the cooling/heating energy, which is required to keep the indoor temperature at 24 °C. The residential building's overall energy usage may be calculated as follows:

$$\dot{E}_{total} = \dot{E}_{HP} + \dot{E}_{beasline} \quad (11)$$

In Equation (11), $\dot{E}_{HP}$ refer to the energy requirement of heat pump express in kWh to keep the indoor temperature at 24 °C, which depend on the outdoor weather. $\dot{E}_{baseline}$ is the baseline load of the house that is independent of the outdoor conditions. This load accounts for plug-in load such as lighting, computers, TV, etc.

$$\begin{aligned} \rho_a C_a V \frac{dT_{h,b}}{dt} &= -\dot{Q}_{lost} + \dot{Q}_{HP} \quad \text{in heating mode} \\ \rho_a C_a V \frac{dT_{c,b}}{dt} &= \dot{Q}_{gain_c} - \dot{Q}_{HP} \quad \text{in cooling mode} \end{aligned} \quad (12)$$

In Equation (12), $Q_{\cdot lost}$ and $\dot{Q}_{gain_c}$ are the heating lost/gain due to conduction, convection, and ventilation express in kWh. $T_{h,b}$ and $T_{C,b}$ are house indoor temperature during cold and summer months, respectively. Other parameters presented in Equation (12) indicates the air density $\rho_a$, the volume of the house (V), and the specific heat capacity of air $C_a$.

### 3.5. System Cost Model

This section describes in detail the economic model used to estimate the total annual cost, which is calculated as the sum of the loan payment and annual operating cost. The capital cost of the proposed system shown in Equation (13) comprises the capital and insulation cost of purchasing a photovoltaic hybrid thermal system, the cost of direct contact membrane desalination, the annual cost for the auxiliary heating system, and the initial cost of the absorption chiller.

$$C_c = PVT_{cost} + DCMD_{cost} + CC_{Hx} + Q_{abs-chiler} \quad (13)$$

The initial system capital cost is treated as an investment that is returned with a fixed-interest loan. The loan periods considered in this study is 20 years. Equation (14) shows the annual loan payment [32].

$$Annual\ Loan\ Payment = C_c * i * (1+i)^n / \left((1+i)^n - 1\right) \quad (14)$$

The overall annual operating cost can be expressed in Equation (15) [28].

$$ATotal\ Cost = Annual\ Loan\ Payment + Annual\ Grid\ Cost - Annual\ Grid\ Sell \quad (15)$$

Table 2 shows the variables considered when calculating the cost of a system. It also includes the study's unit prices (along with references).

**Table 2.** The hybrid system's cost details and house's characteristics used in the simulation.

| Components | Parameters | Value | Ref |
|---|---|---|---|
| PVT | Capital and installed cost | 1800 [$/kW] | [33] |
| | Replacements | 1800 [$/kW] | - |
| | O&M | 5% of total capital cost | [33] |
| | Lifetime | 25 [years] | - |
| Membrane cost | Capital | 50 [$/m$^2$] | - |
| | Replacements | 50 [$/m$^2$] | - |
| | O&M | 1200 [$/year] | - |
| | Lifetime | | |
| Absorption chiller | Capital | 1800 [$/ton] | [34] |
| Geometrical and energy characteristics of a house | Floor Area | 320 m$^2$ | |
| | overall heat transfer coefficient $U_{Wall}$ | 0.34 $[W/m^2 \cdot K]$ | [35] |
| | overall heat transfer coefficient $U_{roof}$ | 0.2 $W/m^2 \cdot K$ | |
| | Electric plug load | 3.5 $W/m^2$ | |
| | Lighting Power Density | 4 $W/m^2$ | |
| | Window-to-Wall Ratio | 15% | |
| Parameters used for evaluating the performance of the proposed system | Energy consumption to supply m$^3$ of water from nearest desalination plant to the selected location | 14 kWh | [36] |
| | Emission due to water transport | 5 kg/m$^3$ | [36] |
| | Electricity price | 0.08 $/kWh | [19] |
| | Electricity sells to grid | 0.05 $/kWh | - |

*3.6. Validation*

Mathematical model for the used DCMD device was validated using experimental data reported in the literature [26]. Figure 4 shows the results of the developed model against the experimental data. Generally, the model showed a good agreement with the experimental results. The model-predicted under various operating conditions for the permeate mass flux, the hot water temperature outlet, and the cold-water temperature outlet were within ±15, ±5, and ±7 division bands, respectively. The origin of deviations might be attributed to two reasons: (i) the variability of the experimental results, and (ii) the model's assumptions.

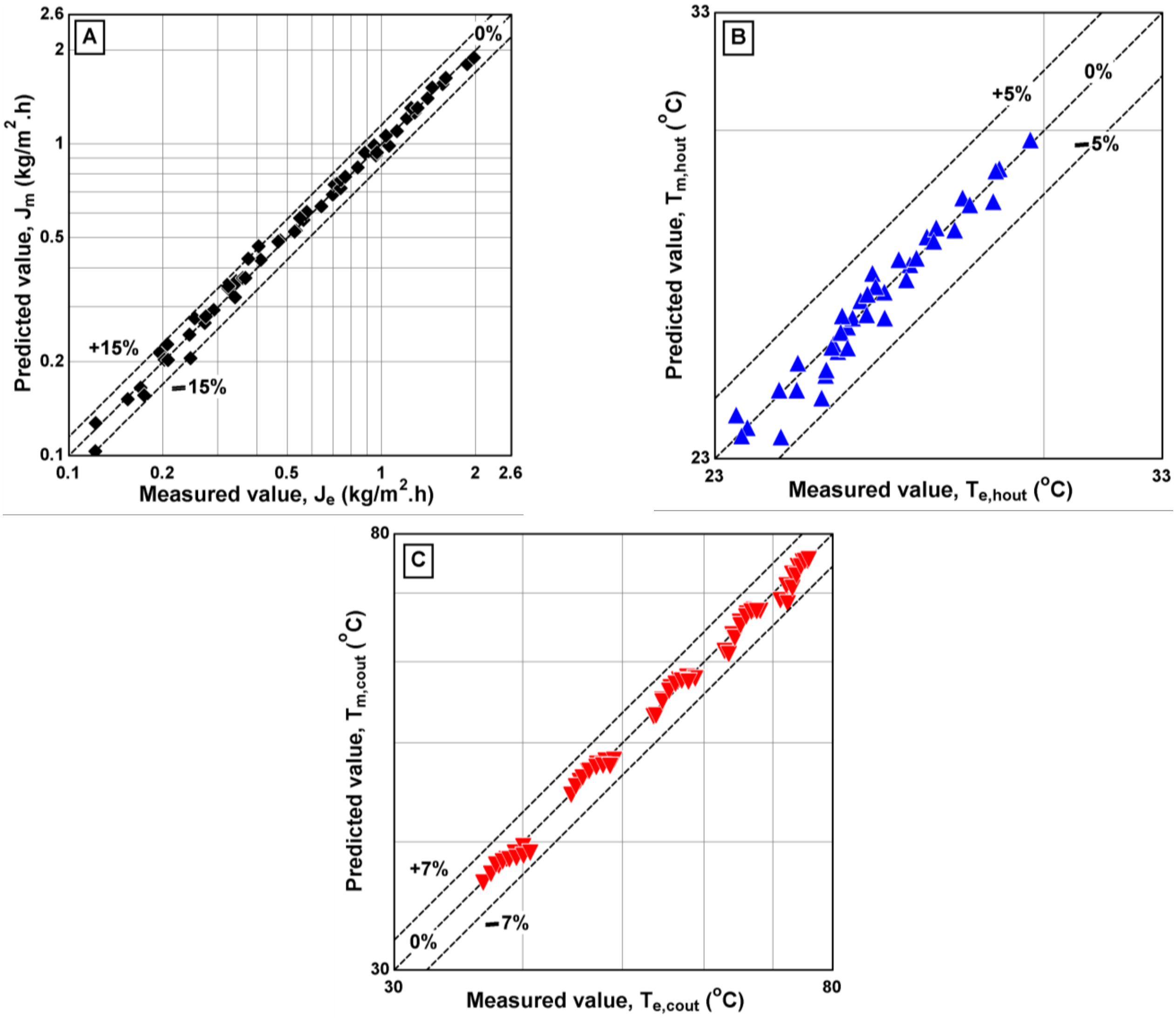


**Figure 4.** Comparison between experimental and model results of the DCMD module (**A**) Permeate mass flux, (**B**) Outlet of hot water temperatures, and (**C**) Outlet of cold-water temperatures.

The energy consumption of the physics model of a residential building that was created was compared to benchmark data from [35], which indicated energy intensities for Saudi Arabia's middle area. The average energy intensity for residential buildings was found to be 136 kWh/m$^2$·year. The physics-based model developed in this study has an energy intensity of 148 kWh/m$^2$. In addition, the PVT model developed previously in prior research was utilized in this work [28].

### 3.7. Solution Algorithm

The proposed hybrid system was evaluated using typical Riyadh, Saudi Arabia weather conditions. Figure 5 depicts in detail the solution procedures utilized in this study. The first step in the simulation is to estimate the hourly electricity and hot water production from the PVT. In this case, the electricity production obtained from the PVT is dispatched to the house for immediate use or sold to the grid if the electricity production is more than house electric demand. The hot water stream is supplied from the storage tank to the DCMD unit, and the portable clean water is sent to residents. The rejected cold water comes from the DCMD is sent back to the chiller to be used for a regenerative purpose. The end goal of this simulation is to optimize the hybrid PVT size by minimizing the annual operating cost and maximizing water productivity. In this case, the proposed hybrid system was optimized using MATLAB built-in function gamultiobj to minimize the total operating cost expressed in Equation (15) and maximize the water yields from the DCMD.

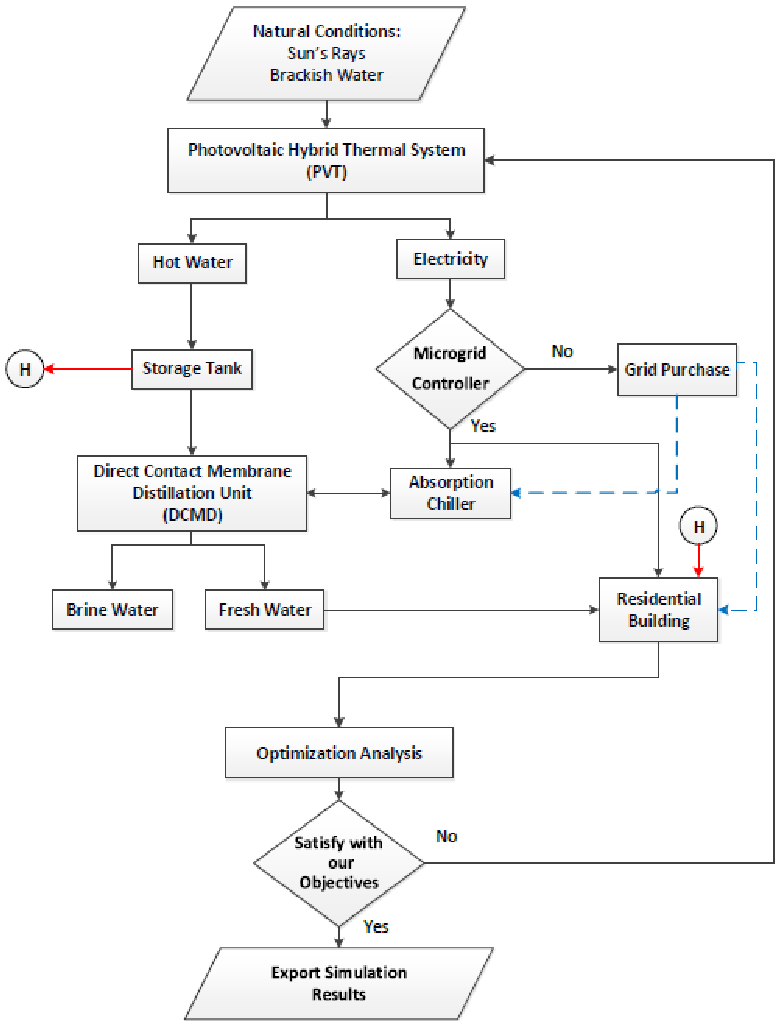


**Figure 5.** Algorithm diagram for solution.

The inputs parameters used to solve the mathematical model is illustrated in Table 3. The flow rate to the DCMD and hot and cold-water temperature varies from maximum and minimum values. Similarly, the number of PVT panels connected in serious and parallel configuration ranges from 5 to 25. These values have a tremendous impact on the levelized cost of water $\frac{\$}{m^3}$. Thus, these variables were optimized to minimize the total operating cost. The ambient conditions implemented in this study are presented in Figure 6.

**Table 3.** Parameters used in the simulation.

| Parameter | Value | |
|---|---|---|
| | **Minimum** | **Maximum** |
| Direct contact membrane distillation (DCMD) | | |
| Mass flow rate $(Q)$ L/hr. | 100 | 300 |
| Hot stream water fed to DCMD $(T_{hot})$ | 40 | 90 |
| Hot stream water fed to DCMD $(T_{cool})$ | 20 | 25 |
| PVT panels | | |
| Number of panels connected in series $(N_s)$ | 5 | 25 |
| Number of panels connected in parallel $(N_p)$ | 5 | 25 |
| Effective absorptance of collector absorber $(\alpha)$ | 0.95 | |
| Transmittance of collector cover system.one glass $(\tau)$ | 0.92 | |
| Temperature coefficient of solar cell efficiency $k^{-1}$ $(B_r)$ | 0.0044 | |
| Reference efficiency from datasheet for standard test conditions using reference temp. of Tr = 25 Celcius (°C) | 25 | |
| Specific heat J/kg K $C_p$ | 4200 | |
| Area of collector $(A_c)$ | 1.3 | |
| Input collector fluid temperature assumed constant $T_{fi}$ | 27 | |
| Ambient temperature Photovoltaic/Thermal System Studies $T_a$ | Varies depend on weather conditions | |
| Solar radiation per unit area absorbed at absorber surface $(S)$ | Varies depend on weather conditions | |

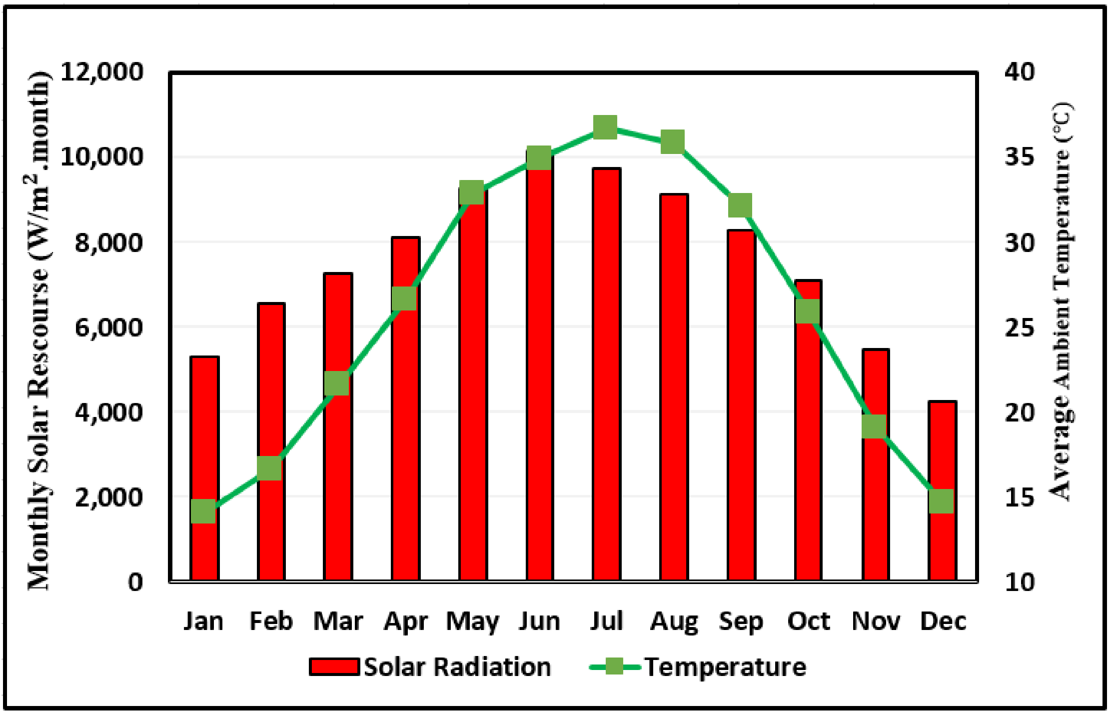


**Figure 6.** Weather condition for the selected location showing Global horizontal irradiance vs. ambient temperature.

## 4. Results and Discussion

The performance of the proposed system was simulated based on a typical weather condition for the city of Riyadh, Saudi Arabia. The hourly variation of the solar radiation and ambient temperature is illustrated in Figure 6. There are wide variations of the ambient temperature and solar radiation during months. It is clear from this figure that the amount of solar radiation in the month of July in the city of Riyadh is abundant. The maximum outdoor solar radiation reaches around 9000 W/m$^2$·month. Because the hybrid system is powered by solar energy, and since the amount of solar energy for the selected city is rich, this figure reveals a sustainable opportunity for the proposed system presented in this study.

Figure 7 depicts the specific cost of water (SCW) for the proposed system over a wide range of the DCMD membrane surface areas. For small membrane areas, the SCW is considerably high because there is an inadequate heat transfer surface available for heat transmission across the hydrophobic membrane. It was observed that increasing the membrane surface area reduces the SCW. For a larger membrane area, the SCW is fairly stable. Thus, increasing the membrane area leads to a higher production rate, but the overall cost has a marginal impact due to the rise in operating costs.

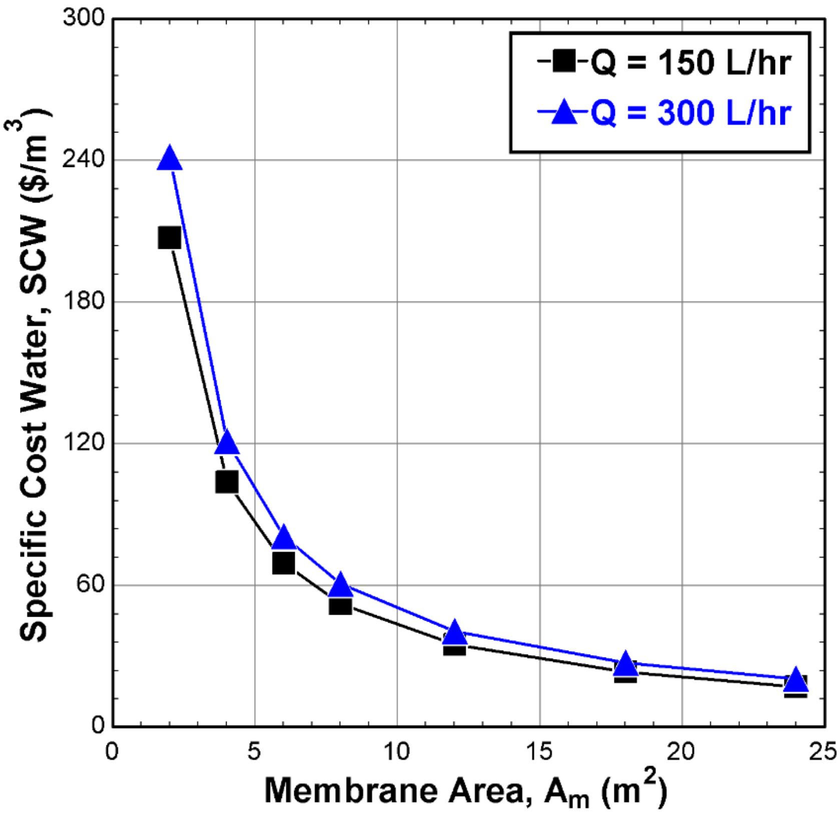


**Figure 7.** Effect of membrane area on Specific Cost Water (SCW) for different flow rates.

One of the parameters that influence the overall SCW is the inlet temperature of the brackish water to the collectors. Figure 8 shows the variation of inlet water temperature to the collectors and its impact on the overall SCW. Figure 8 depicts that the SCW was substantially dependent on the inlet water temperature to the collectors. With a fixed amount of flow rate, the SCW was reduced by 4.5% as a result of increasing the increment of the inlet water temperature by 5 °C.

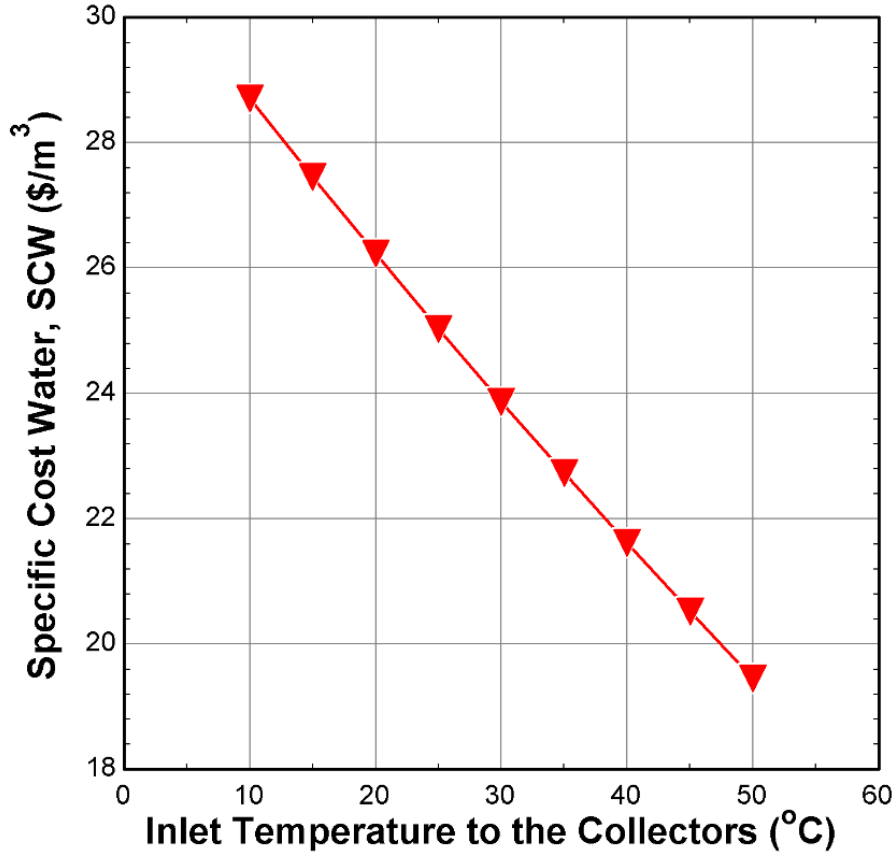


**Figure 8.** Effect of inlet water temperature to the collectors on SCW. The triangles represent the specific cost water values under the variation of collectors' temperature.

Auxiliary heating was utilized in the proposed system in case the solar energy gained by the collector is not sufficient to raise the brackish water to a predetermined temperature. Figure 9 illustrates the annual auxiliary heating energy required as a function of the number of panels connected in series in two different situations. The bottom two lines (black square and blue triangle) depict the annual auxiliary during daylight for two different flow rates. In this case, the DCMD was only operating during sunlight. The other two lines (green circle and red diamond) represent the annual auxiliary heating requirement when continuous water production is required. It is clear from this figure a continuous water production increases the annual auxiliary heating for a given number of panels by 49%.

Figure 10 depicts the overall performance of the proposed optimized system. It shows the monthly energy electricity produced by the PVT, monthly electricity sells to the grid, and the imported electricity from the grid. As it is shown in this figure, the energy-saving in cold months is substantially higher as compared with summer months. The reason for this is that air conditioning account for about 70% of energy consumption in residential buildings. In this case, the proposed system is producing more electricity than the house's demand in the winter seasons.

For continuous water production, the proposed system costs 5% more for each cubic meter. This is illustrated in Figure 11. This figure shows the SCW of water as a function of the panels connected in series. It is clear from this figure that the best price occurs at Ns = 18. At lower panels connect in series, the SCW is high because more auxiliary heating is used to rise the water temperature to 70 °C. Conversely, increasing the number of panels beyond 18 rises the SCW due to the increase in operating and insulation cost.

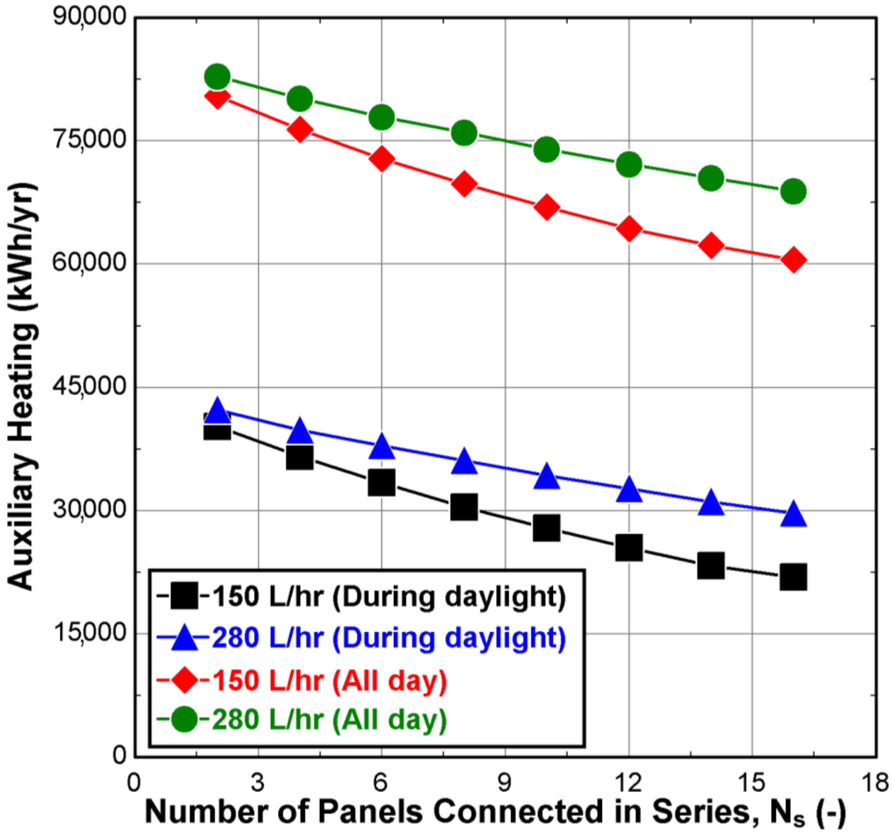


**Figure 9.** Annual auxiliary heating as function of number of panels and mass flow rate.

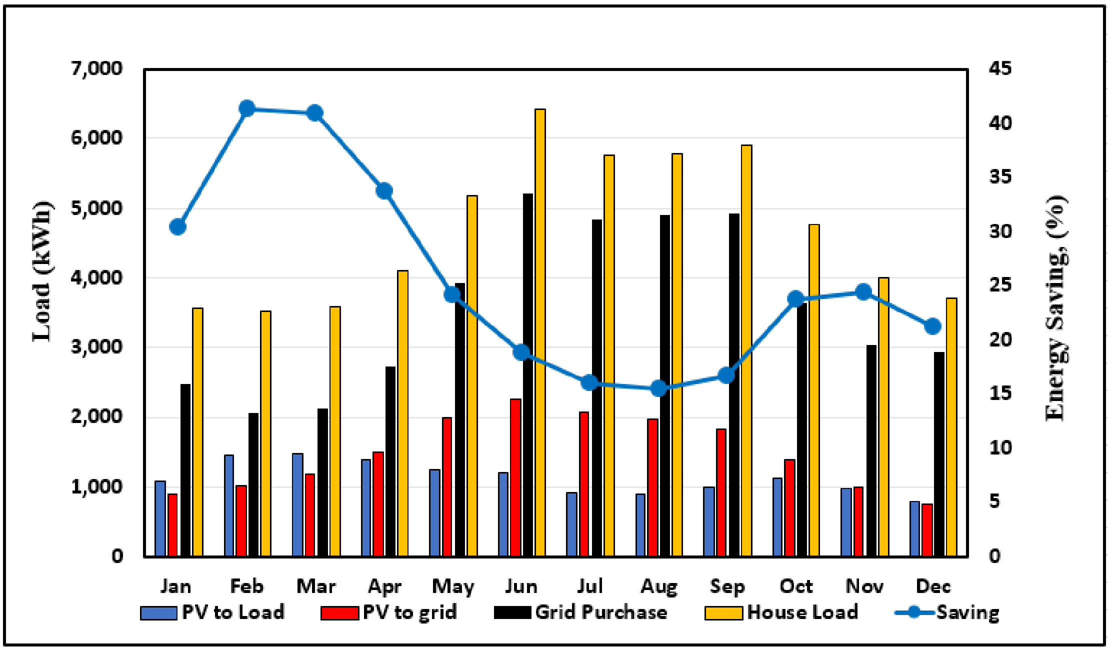


**Figure 10.** Monthly power generation of PVT, load demand, and exported and imported grid power to the house, and overall energy saving.

Almost all energy required in a residential building in Saudi Arabia comes from nonrenewable sources. In addition, most of desalinated water for residents in the Riyadh region is transported from Jubail and Ras Al-Khair plants [36], which are 500 km away. The environmental and energy cost for such transportation is high. It was reported by other researchers that the energy required to transport 1 m$^3$ of desalinated water from the nearest desalination plant is 14 kWh/m$^3$, which is equivalent to 5 kg $CO_2$/m$^3$ [36]. Thus, decentralized water is imperative. Figure 12 shows the results of the optimized system. The annual $CO_2$ saving for a single residential building is 4300 kg as a result of decentralized water and energy.

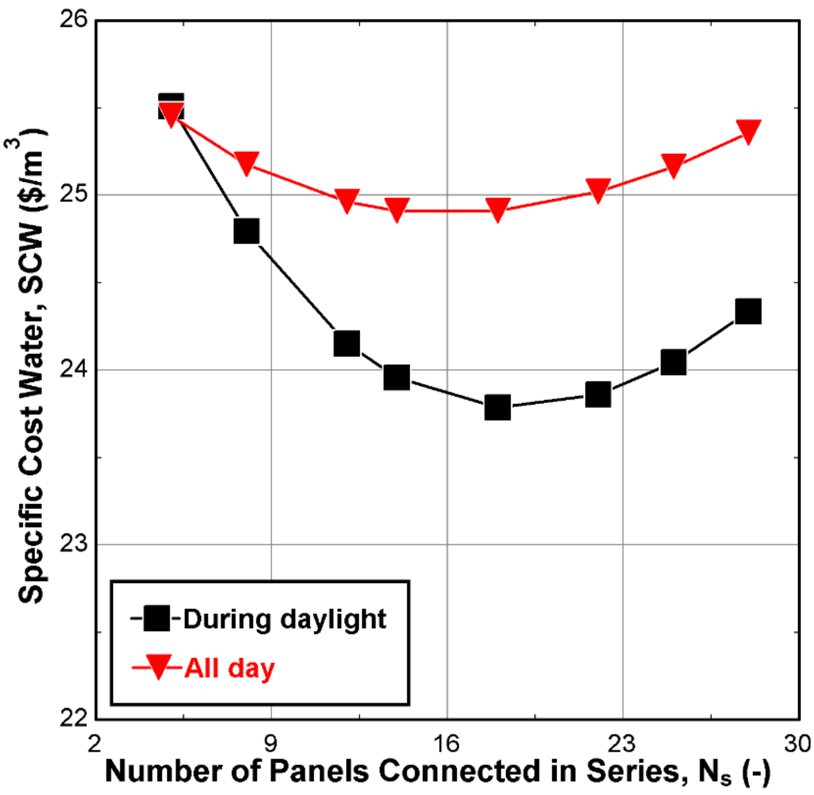


**Figure 11.** The SCW at different number of panels connected in series.

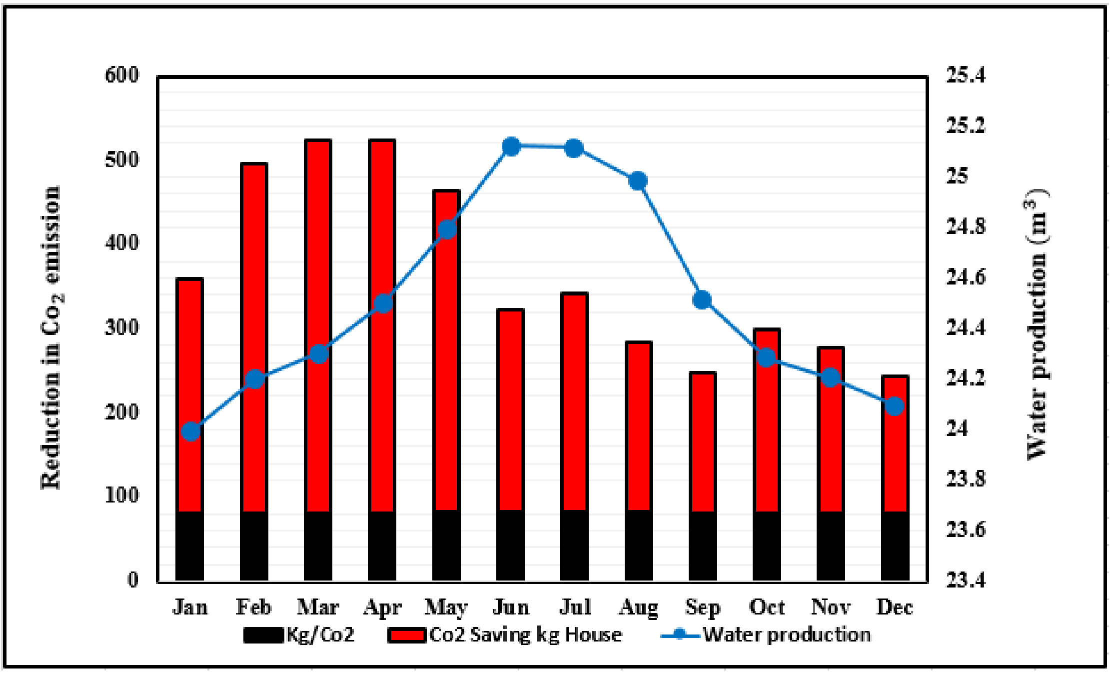


**Figure 12.** Environmental analysis and monthly water production.

The capital and investment costs of the proposed system have a significant impact on the SCW. The impact of the PVT system's capital cost and the cost of auxiliary heating on the SCW was investigated using a sensitivity analysis, as shown in Figure 13. As mentioned previously, auxiliary heating is used to ensure the hot feed water to the DCMD unit to not fall below 70 °C. It is clear from Figure 13 that the SCW is proportional to both PVT capital price and the auxiliary heating cost. It is worth noting that the average price for the PVT is 1800 $/kW. With current market price, the SCW for the proposed system is 23.6 $/m$^3$. In addition, previous studies show that the cost of desalinated water (SCW) varies from 15 to 18.34 $/m$^3$ [16,17]. These studies utilized membrane technology powered by solar energy on a small scale. The simulated results obtained from the proposed system are comparative to previous studies where the where SCW is around 23.6 $/m$^3$.

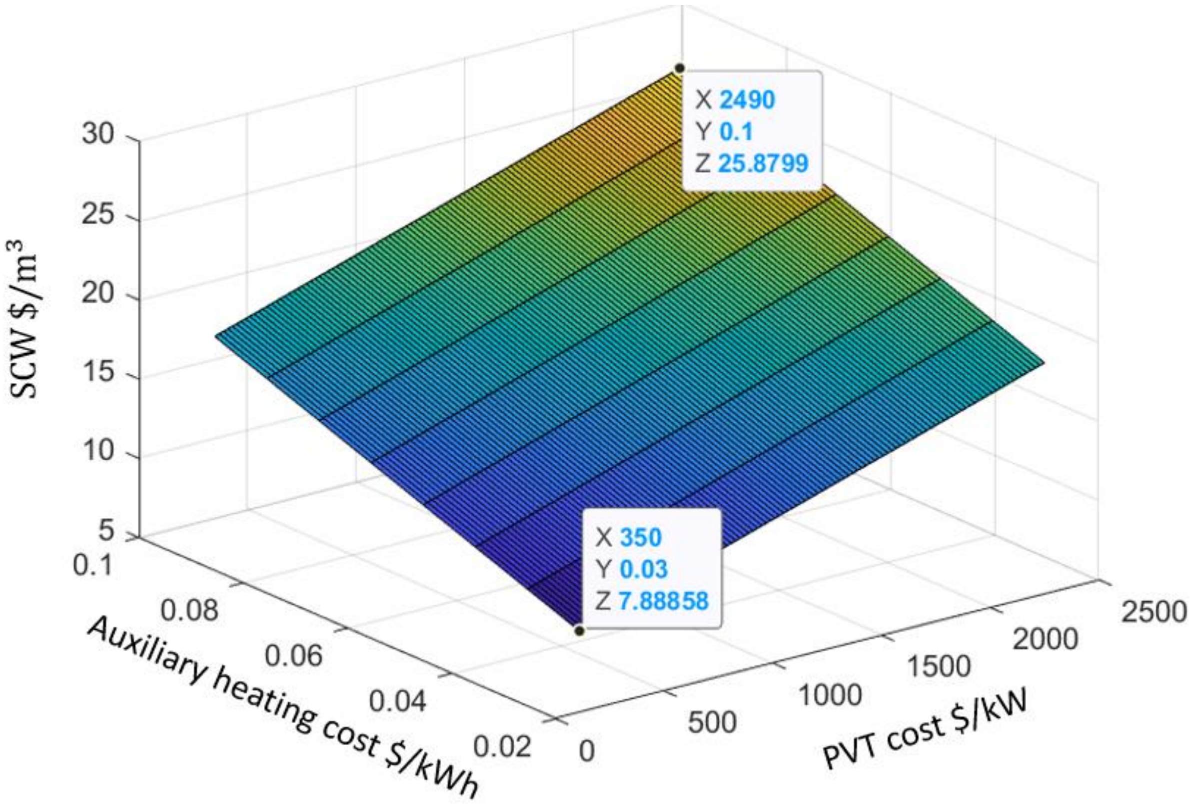


**Figure 13.** The sensitivity of varying PVT capital and installation cost and the required auxiliary heating on the SCW.

## 5. Conclusions

This research evaluates the performance of a direct contact membrane desalination system integrated with PVT modules for the continuous generation of electricity and clean water. The proposed system's optimal design that leads to minimum operating cost is investigated, and a detailed techno-economic analysis of the specific cost of water is examined under different scenarios. Other parameters that affect the performance of the proposed system such as the rated capacity of PVT, mass flow rate to the DCMD, the inlet feed water temperature to the collectors, were explored. The following are the main conclusions:

(1) The proposed system has the capacity to provide a small family with clean portable water. The average monthly freshwater production is 23.6 m$^3$/month based on a typical meteorological weather data for Riyadh, Saudi Arabia. Given an average daily water consumption per capita in Saudi Arabia of 250 L/day [37], the proposed system can meet daily water requirements for 3–4 people.

(2) The annual operating cost for the proposed system is \$5300. This cost includes the annual loan payment and the energy purchased from the grid. The specific cost of water (SCW) is 23.6 $\$/m^3$. At a small-scale desalination system, the proposed system in this study is attractive from an economic and environmental perspective when compared with conventional systems.
(3) For microgrid integration, the lowest operating cost was found at 25% renewable energy penetration. This means that the proposed hybrid system is capable of meeting 25% of the residential building's electric load. The ability of the proposed system to cover higher energy demand for the residential building is limited due to the need for energy storage. In this case, increasing the annual renewable energy penetration above 25 percent results in a higher operating cost. This was ascribed to significant capital expenditures as a result of the system's oversizing.
(4) Environmental benefits of the proposed system are crucial as it eliminates energy consumption from pipelines that used to transport clean water from the nearest desalination plant. The annual $Co_2$ emission reduction for a single building is 4300 kg.

**Author Contributions:** Conceptualization, F.A.A. and A.N.; methodology, F.A.A.; software, F.A.A.; validation, F.A.A. and A.N.; formal analysis, A.N. and J.O.; investigation, E.A. and H.A.-A.; resources, A.N.; data curation, A.N.; writing—original draft preparation, F.A.A.; writing—review and editing, E.A., H.A.-A. and J.O.; visualization, E.A. and H.A.-A.; supervision, E.A.; project administration, F.A.A.; funding acquisition, F.A.A. All authors have read and agreed to the published version of the manuscript.

**Funding:** The authors extend their appreciation to the Researches Supporting Project number (RSP2022R515), King Saud University, Riyadh, Saudi Arabia, for funding this research work.

**Institutional Review Board Statement:** Not Applicable.

**Informed Consent Statement:** Not Applicable.

**Data Availability Statement:** Not Applicable.

**Conflicts of Interest:** The authors declare no conflict of interest.

## Nomenclature

| | |
|---|---|
| $\dot{Q}_{h,N_s}$ | thermal energy transmitted to the working fluid |
| $A_c$ | Collector area |
| $F_R$ | Heat removal factor |
| $S$ | Solar radiation |
| $N_S$ | Number of panels connected in series |
| $N_p$ | Number of panels connected in parallel |
| $U_L$ | Heat losses through conductance |
| $T_{fi}$ | Fluid inlet temperature |
| $T_a$ | Ambient temperature |
| $m$ | Mass flow rate |
| $C_p$ | Specific heat |
| $Q_{e,total}$ | Electric energy produced by PVT |
| V | Volume of the house |
| $\dot{Q}_{aux}$ | Auxiliary heating |
| $T_{h,b}$ | House indoor temperature during cold months |
| $T_{c,b}$ | House indoor temperature during summer months |
| $Q_{lost}$ | heating lost due to conduction, convection, and ventilation |
| $Q_{gain\_c}$ | heating gains due to conduction, convection, and ventilation |
| $PVT_{cost}$ | Capital cost for the PVT |
| $Q_{abs-chiler}$ | Absorption chiller capital cost |

**Greek**

$\eta_c$ Electric efficiency
$\alpha$ collector absorptance

## References


1. Report: Universal Access to Sustainable Energy Will Remain Elusive Without Addressing Inequalities. World Bank. Available online: https://www.worldbank.org/en/news/press-release/2021/06/07/report-universal-access-to-sustainable-energy-will-remain-elusive-without-addressing-inequalities (accessed on 6 August 2022).
2. Facts and Statistics | WaterAid. Available online: https://www.wateraid.org/facts-and-statistics (accessed on 6 August 2022).
3. Ferroukhi, R.; Nagpal, D.; Lopez-Peña, A.; Hodges, T.; Mohtar, R.H.; Daher, B.; Mohtar, S.; Keulertz, M. *Renewable Energy in the Water, Energy & Food Nexus*; IRENA: Abu Dhabi, United Arab Emirates, 2015; pp. 1–125.
4. Seznec, D.J.-F.; Mosis, S. The Energy Transition in the Arab Gulf: From Vision to Reality. p. 26. Available online: https://www.atlanticcouncil.org/wp-content/uploads/2021/08/AC_GulfTransitions_FINAL.pdf (accessed on 20 August 2022).
5. Energy & Sustainability. Vision 2030. Available online: https://www.vision2030.gov.sa/thekingdom/explore/energy/ (accessed on 17 July 2021).
6. Krarti, M.; Dubey, K.; Howarth, N. Evaluation of building energy efficiency investment options for the Kingdom of Saudi Arabia. *Energy* **2017**, *134*, 595–610. [CrossRef]
7. Demirbas, A.; Hashem, A.A.; Bakhsh, A.A. The cost analysis of electric power generation in Saudi Arabia. *Energy Sources Part B Econ. Plan. Policy* **2017**, *12*, 591–596. [CrossRef]
8. Chen, Q.; Burhan, M.; Akhtar, F.H.; Ybyraiymkul, D.; Shahzad, M.W.; Li, Y.; Ng, K.C. A decentralized water/electricity cogeneration system integrating concentrated photovoltaic/thermal collectors and vacuum multi-effect membrane distillation. *Energy* **2021**, *230*, 120852. [CrossRef]
9. Krnac, A.; Araiz, M.; Rana, S.; Velardo, J.; Date, A. Investigation of Direct Contact Membrane Distillation coupling with a Concentrated Photovoltaic solar system. *Energy Procedia* **2019**, *160*, 246–252. [CrossRef]
10. Rahaoui, K.; Ding, L.C.; Tan, L.P.; Mediouri, W.; Mahmoudi, F.; Nakoa, K.; Akbarzadeh, A. Sustainable Membrane Distillation Coupled with Solar Pond. *Energy Procedia* **2017**, *110*, 414–419. [CrossRef]
11. Kim, Y.D.; Thu, K.; Ghaffour, N.; Ng, K.C. Performance investigation of a solar-assisted direct contact membrane distillation system. *J. Membr. Sci.* **2013**, *427*, 345–364. [CrossRef]
12. Shafieian, A.; Khiadani, M. A novel solar-driven direct contact membrane-based water desalination system. *Energy Convers. Manag.* **2019**, *199*, 112055. [CrossRef]
13. Karam, A.M.; Laleg-Kirati, T.M. Real time optimization of solar powered direct contact membrane distillation based on multivariable extremum seeking. In Proceedings of the 2015 IEEE Conference on Control Applications (CCA), Sydney, NSW, Australia, 21–23 September 2015; pp. 1618–1623. [CrossRef]
14. Chen, T.-C.; Ho, C.-D. Immediate assisted solar direct contact membrane distillation in saline water desalination. *J. Membr. Sci.* **2010**, *358*, 122–130. [CrossRef]
15. Banat, F.; Jwaied, N. Economic evaluation of desalination by small-scale autonomous solar-powered membrane distillation units. *Desalination* **2008**, *220*, 566–573. [CrossRef]
16. Li, G.; Lu, L. Modeling and performance analysis of a fully solar-powered stand-alone sweeping gas membrane distillation desalination system for island and coastal households. *Energy Convers. Manag.* **2020**, *205*, 112375. [CrossRef]
17. Zhang, L.-Z.; Li, G.-P. Energy and economic analysis of a hollow fiber membrane-based desalination system driven by solar energy. *Desalination* **2017**, *404*, 200–214. [CrossRef]
18. Al-Sharafi, A.; Sahin, A.Z.; Ayar, T.; Yilbas, B.S. Techno-economic analysis and optimization of solar and wind energy systems for power generation and hydrogen production in Saudi Arabia. *Renew. Sustain. Energy Rev.* **2017**, *69*, 33–49. [CrossRef]
19. Alharthi, Y.Z.; Siddiki, M.K.; Chaudhry, G.M. Resource Assessment and Techno-Economic Analysis of a Grid-Connected Solar PV-Wind Hybrid System for Different Locations in Saudi Arabia. *Sustainability* **2018**, *10*, 3690. [CrossRef]
20. Baseer, M.A.; Alqahtani, A.; Rehman, S. Techno-economic design and evaluation of hybrid energy systems for residential communities: Case study of Jubail industrial city. *J. Clean. Prod.* **2019**, *237*, 117806. [CrossRef]
21. Rehman, S.; Alam, M.M.; Meyer, J.P.; Al-Hadhrami, L.M. Feasibility study of a wind–pv–diesel hybrid power system for a village. *Renew. Energy* **2012**, *38*, 258–268. [CrossRef]
22. Mustafa, J.; Almehmadi, F.A.; Alqaed, S. A novel study to examine dependency of indoor temperature and PCM to reduce energy consumption in buildings. *J. Build. Eng.* **2022**, *51*, 104249. [CrossRef]
23. Alqaed, S.; Mustafa, J.; Almehmadi, F.A. The effect of using phase change materials in a solar wall on the number of times of air conditioning per hour during day and night in different thicknesses of the solar wall. *J. Build. Eng.* **2022**, *51*, 104227. [CrossRef]
24. Technology | SolarSpring. 19 March 2021. Available online: https://solarspring.de/en/technology/ (accessed on 6 August 2022).
25. Ali, E.; Orfi, J.; Najib, A. Developing and validating a dynamic model of water production by direct-contact membrane distillation. *PLoS ONE* **2020**, *15*, e0230207. [CrossRef]
26. Najib, A.; Orfi, J.; Ali, E.; Saleh, J. Thermodynamics analysis of a direct contact membrane distillation with/without heat recovery based on experimental data. *Desalination* **2019**, *466*, 52–67. [CrossRef]

27. R: The R Project for Statistical Computing. Available online: https://www.r-project.org/ (accessed on 22 February 2022).
28. Alqaed, S.; Mustafa, J.; Almehmadi, F.A. Design and Energy Requirements of a Photovoltaic-Thermal Powered Water Desalination Plant for the Middle East. *Int. J. Environ. Res. Public Health* **2021**, *18*, 1001. [CrossRef]
29. Dubey, S.; Tiwari, G.N. Analysis of PV/T flat plate water collectors connected in series. *Sol. Energy* **2009**, *83*, 1485–1498. [CrossRef]
30. Florschuetz, L.W. Extension of the Hottel-Whillier model to the analysis of combined photovoltaic/thermal flat plate collectors. *Sol. Energy* **1979**, *22*, 361–366. [CrossRef]
31. Labus, J.; Bruno, J.C.; Coronas, A. Performance analysis of small capacity absorption chillers by using different modeling methods. *Appl. Therm. Eng.* **2013**, *58*, 305–313. [CrossRef]
32. Soheyli, S.; Mayam, M.H.S.; Mehrjoo, M. Modeling a novel CCHP system including solar and wind renewable energy resources and sizing by a CC-MOPSO algorithm. *Appl. Energy* **2016**, *184*, 375–395. [CrossRef]
33. Gabrielli, P.; Gazzani, M.; Novati, N.; Sutter, L.; Simonetti, R.; Molinaroli, L.; Manzolini, G.; Mazzotti, M. Combined water desalination and electricity generation through a humidification-dehumidification process integrated with photovoltaic-thermal modules: Design, performance analysis and techno-economic assessment. *Energy Convers. Manag.* **2019**, *1*, 100004. [CrossRef]
34. Absorption Chillers for CHP Systems. p. 4. Available online: https://www.energy.gov/eere/amo/downloads/absorption-chillers-chp-systems-doe-chp-technology-fact-sheet-series-fact-sheet (accessed on 7 March 2022).
35. Krarti, M.; Aldubyan, M.; Williams, E. Residential building stock model for evaluating energy retrofit programs in Saudi Arabia. *Energy* **2020**, *195*, 116980. [CrossRef]
36. Alnajdi, O.; Wu, Y.; Calautit, J.K. Toward a Sustainable Decentralized Water Supply: Review of Adsorption Desorption Desalination (ADD) and Current Technologies: Saudi Arabia (SA) as a Case Study. *Water* **2020**, *12*, 1111. [CrossRef]
37. Per Capita Water Consumption in Saudi Regions during the Period 2009–2017. Available online: https://www.stats.gov.sa/sites/default/files/per_capita_water_consumption_in_saudi_regions_en_0.pdf (accessed on 17 March 2022).